A EUROPEAN JOURNAL OF CHEMICAL BIOLOGY

CHEMBIOCHEM

SYNTHETIC BIOLOGY & BIO-NANOTECHNOLOGY

Accepted Article

Title: Effect of alternative redox partners and oxidizing agents in CYP154C8 catalytic activity and product distribution

Authors: Bikash Dangi, Hyun Park, and Tae-Jin Oh

To be cited as: *ChemBioChem* 10.1002/cbic.201800284

Link to VoR: http://dx.doi.org/10.1002/cbic.201800284

A Journal of ChemPubSoc Europe

WILEY-VCH

www.chembiochem.org

Effect of alternative redox partners and oxidizing agents in CYP154C8 catalytic activity and product distribution

Bikash Dangi[1], Hyun Park[2,3], Tae-Jin Oh[1,4,5,*]

[1]*Department of Life Science and Biochemical Engineering, SunMoon University, 70 Sunmoon-ro 221, Tangjeong-myeon, Asan-si, Chungnam 31460, Republic of Korea*

[2]*Unit of Polar Genomics, Korea Polar Research Institute, Incheon 21990, Republic of Korea*

[3]*Department of Polar Sciences, University of Science and Technology, Incheon 21990, Republic of Korea*

[4]*Department of Pharmaceutical Engineering and Biotechnology, SunMoon University, 70 Sunmoon-ro 221, Tangjeong-myeon, Asan-si, Chungnam 31460, Republic of Korea*

[5]*Genome-based BioIT Convergence Institute, 70 Sunmoon-ro 221, Tangjeong-myeon, Asan-si, Chungnam 31460, Republic of Korea*

Author for correspondence: Prof. Tae-Jin Oh

Tel: +82(41)530-2677;

Fax: +82(41)530-2279;

E-mail: tjoh3782@sunmoon.ac.kr

Running title: Steroid hydroxylation of CYP154C8 depend on electron transport system

Abstract

CYP154C8 catalyzes the hydroxylation of diverse steroids as was previously demonstrated by using an NADH-dependent system that included putidaredoxin and putidaredoxin reductase as redox partner proteins carrying electrons from NADH. In other reactions, CYP154C8 reconstituted with spinach ferredoxin and NADPH-dependent ferredoxin reductase, displayed an altered catalytic activity compared with the NADH-dependent system. The NADPH-dependent system showed multi-step oxidation of progesterone and other substrates including androstenedione, testosterone and nandrolone. (Diacetoxyiodo)benzene is employed to generate compound I (FeO^{3+}) actively supporting the redox reactions catalyzed by CYP154C8. In addition to 16α-hydroxylation, progesterone and 11-ketoprogesterone were also hydroxylated at the respective 6β position in the reaction supported by (diacetoxyiodo)benzene. CYP154C8 was active in the presence of high concentration (>10 mM) of H_2O_2, although surprisingly, the optimum conversion was achieved at ~75 mM H_2O_2. More importantly, H_2O_2 tolerance of CYP154C8 showed a very low heme oxidation rate constant (*K*) even at high concentrations of H_2O_2. Our results demonstrate that the alternative redox partner and oxidizing agents influence the catalytic efficiency and product distribution of a cytochrome P450 enzyme. More importantly, such choice affected the type and selectivity of the reaction catalyzed by the P450 enzyme.

Keywords: Cytochrome P450; (diacetoxyiodo)benzene; electron transport system; hydrogen peroxide; steroid hydroxylation.

Introduction

Cytochrome P450s (CYPs) are widely distributed in all forms of life (archaea, bacteria and eukarya) (1). Most CYP catalyzes the oxidative reaction utilizing O_2 and two electrons supplied by NAD(P)H and transferred via redox partners like flavin-containing reductase and iron-sulfur ferredoxins (2). The mammalian CYPs are membrane bound and reduced by NADPH-cytochrome P450 reductase (CPR), which is also a membrane-bound enzyme required for electron transfer from NADPH to CYPs in the endoplasmic reticulum. The FAD- and FMN-containing CPRs support CYPs of the class of II (3). The class I redox system includes bacterial and mitochondrial iron-sulfur (Fe-S) containing proteins (ferredoxin/adrenodoxin, Fdx/Adx) and FAD reductase (ferredoxin/adrenodoxin reductase, Fdr/Adr). In addition, flavin-dependent proteins called flavodoxins (flavin mononucleotide containing proteins) are present in some prokaryotic organisms and certain algae (4). A distinct group is built by the so-called self-sufficient CYP in which a CPR-like reductase domain is fused to a monooxygenase domain (5-11). One of the well-known forms is P450BM3 (CYP102A1) discovered in *Bacillus megaterium*, a natural fusion of fatty acid hydroxylase P450 to a soluble CPR (5). In addition to CYPs that are either linked to electron carrier proteins or require redox partner proteins to receive electrons from reducing equivalent, a few unusual CYPs (CYP170A1, CYP154A1 and CYP170A1) have been characterized with activity in the absence of redox partners (12-14). Only a few native CYPs have been found to display peroxygenase and peroxidase functions, catalyzing the peroxygenation of various substrates in the presence of H_2O_2 and other peroxy compounds (15-20). Using the 'peroxide shunt' pathway, ferric CYP is directly moved into ferric hydroperoxo intermediate known as compound 0. The H_2O_2-shunt reaction is an attractive option for monooxygenation reactions by CYP enzymes because these reactions are independent of redox

partner proteins and more importantly a low-cost of H_2O_2 can be significant on an industrial scale. Many efforts have been made to develop artificial H_2O_2-dependent CYPs considering their benefit as a practical biocatalyst (21-23). In addition, the H_2O_2-dependent CYPs have been deployed to oxidize non-native substrate in the presence of decoy molecules (20, 24-25). Further, single oxygen donors (e.g., periodate and iodosobenzene) are also found to promote CYP-catalyzed monooxygenation reactions, resulting in a highly reactive ferryl heme π-cation radical, compound I (26-29). However, a few CYPs are known to display such characteristics in the presence of specific chemical compounds. The characterization or synthetic application of CYPs has often been mediated via one or more surrogate redox partners either in an isolated form or after artificial fusion with CYP complex, due to the difficulty in obtaining native redox partners (30-34). It is generally believed that the choice of the surrogate partners or their mode of action does not affect the type and selectivity of the reactions catalyzed by CYPs (35). However, the alternative redox partners might influence the catalytic efficiency and the product distribution (29, 35-40).

CYPs like CYP106A1, CYP106A2, CYP109B1, CYP109E1, CYP154C3, CYP154C5, CYP260A1 and CYP260B1 originated from the bacterial source are known to hydroxylate steroids (32, 33, 41-45). CYP154C8 shows high similarity with CYP154C3 (74%) and CYP154C5 (66%), both of which are reported to hydroxylate steroids at C16α position. CYP154C8 was previously characterized with the NADH-dependent system comprising putidaredoxin reductase (Pdr) and putidaredoxin (Pdx) as redox partner proteins to transfer electrons from NADH to CYP (46). It was found to hydroxylate diverse steroids at different positions. Androstenedione, testosterone and 11-ketoprogesterone steroids were 16α-hydroxylated and two other dihydroxylated products of progesterone were formed as a result of

subsequent hydroxylation of 16α-hydroxyprogesterone by CYP154C8. The major product of corticosterone was found to be 21-hydroxycorticosterone, and substrate bearing hydroxyl or carbonyl group at C11 and C21 position showed similar product formation with corticosterone. In this work, the *in vitro* reactions with steroids (Scheme 1) mediated via NADPH-dependent redox partner system as well as the oxidizing agents (diacetoxyiodo)benzene and H_2O_2 showed changes in product distribution and catalytic activity of CYP154C8 compared with NADH-dependent system. However, other oxidizing agents including sodium periodate, sodium chlorite and tert-butyl hydroperoxide failed to support the *in vitro* reaction catalyzed by CYP154C8.

Materials and methods

Chemical and reagents

All steroid substrates were purchased from Tokyo Chemical Industry Co., Ltd. (Korea). Isopropyl-1-thio-β-$_D$-galactopyranoside (IPTG), 1,4-dithiothreitol (DTT), and kanamycin were obtained from Duchefa Bohemie (Korea). Ampicillin (Amp), chloramphenicol (Cm), α-aminolevulinic acid (ALA), nicotinamide adenine dinucleotide (NADH), nicotinamide adenine dinucleotide phosphate (NADPH), hydrogen peroxide (H_2O_2), (diacetoxyiodo)benzene, cytochrome C, catalase, formate dehydrogenase, glucose-6-phosphate dehydrogenase, glucose-6-phosphate, spinach ferredoxin (Fdx) and spinach ferredoxin reductase (Fdr) were procured from Sigma-Aldrich (Korea). Restriction enzymes were obtained from Takara Clontech (Korea). T4 DNA ligase, DNA polymerase, and dNTPs were supplied by Takara Bio (Japan). All other chemicals were high-grade products obtained from commercially available sources.

Enzymatic *in vitro* assay with NADPH and its surrogate redox partner Fdx and Fdr

The heterologous expression and purification of CYP154C8 was performed as described previously (46). Similarly, the surrogate redox partners, Pdx and Pdr, were expressed and purified as described elsewhere (47). Reaction mixtures contained 3 µM substrate, 3 µM CYP154C8, 6 µM Fdx, 0.1 U Fdr, 10 mM glucose-6-phosphate, 1 U glucose-6-phosphate dehydrogenase, 100 µg/mL catalase, 1 mM $MgCl_2$ and 250 µM NADPH. All the *in vitro* reactions in the enzymatic assay were incubated at 30°C with shaking (200 rpm) for 2 h in 50 mM potassium phosphate buffer containing equal concentrations of substrate (500 µM) and CYP enzyme (3 µM) in a final reaction volume of 0.5 mL. The reactions were extracted twice with 500 µL of ethyl acetate and dried under vacuum. The dried reaction mixture was dissolved in HPLC solvent acetonitrile (70%) and water (30%) for further analysis.

Enzymatic *in vitro* assay with surrogate oxidant

The reactions were initiated separately with the addition of H_2O_2 (biological hydroperoxide) and (diacetoxyidodo)benzene (exogenous oxidant). The *in vitro* activity of CYP154C8 was optimized with different concentrations of H_2O_2 ranging from 0.2 ~ 100 mM, and 1 ~ 5 mM of (diacetoxyidodo)benzene. The data shown here were obtained via *in vitro* reactions that included 75 mM H_2O_2 and 2 mM (diacetoxyidodo)benzene, separately. The reaction mixture (0.5 mL) contained 500 µM steroid substrate and 3 µM CYP154C8 in potassium phosphate buffer (pH 7.4). Reactions were triggered by the addition of H_2O_2 and (diacetoxyidodo)benzene, separately at 30°C for 2 h. The reaction mixture was extracted as described previously (46).

Hydrogen peroxide tolerance of CYP154C8

The hydrogen peroxide tolerance of CYP154C8 was monitored using UV-visible spectroscopy on a Biochrome Libra S35PC spectrophotometer. Oxidative modification of CYP154C8 (3 µM) was carried out in the range of 0.2 ~ 100 mM concentrations of H_2O_2. After the addition of H_2O_2, the absorbance was recorded at a wavelength of 350 ~ 500 nm every 90 s for 30 min at room temperature. The soret peak intensity (417 nm) of CYP154C8 was plotted against time, and the data fitted using one phase decay in GraphPad Prism 6 software to calculate the rate constant for heme oxidation (*K*). Associated absorbance amplitudes (*A*) for heme were calculated as the difference between the highest and the lowest absorbance at soret peak.

Determination of catalytic efficiency and kinetic parameters

The time-dependent *in vitro* conversion of progesterone and 16α-hydroxyprogesterone was carried out using 2 mM (diacetoxyidodo)benzene and 75 mM H_2O_2, respectively. The reaction mixture (500 µL) contained 1 µM CYP154C8 and 500 µM substrate. The reaction was performed at 30°C with shaking (400 rpm) at intervals of 1 ~ 60 min. All the reaction mixture was extracted as described previously, and the conversion (%) of each product at different time intervals was calculated from the area of the product peaks based on HPLC chromatogram. The product concentration with the substrate progesterone and 16α-hydroxyprogesterone in the presence of (diacetoxyido)benzene and 75 mM H_2O_2, respectively, was determined at different substrate concentrations ranging from 25 ~ 400 µM. The reaction mixture was incubated and extracted as described elsewhere. Assuming the absorbance properties of products and substrate

same, the products were quantified by correlating the peak area of the respective product(s) with the combined peak area of product(s) and the substrate.

Product purification and characterization

Large-scale (300 mL) *in vitro* reactions were carried out to determine the structure of the products catalyzed by CYP154C8. The reaction was carried out separately in a 15 mL volume to determine the products obtained in the presence of 2 mM (diacetoxyidodo)benzene. All *in vitro* reactions were carried out in 50 mM potassium phosphate buffer (pH 7.4) for 2 h in the presence of 3 µM CYP154C8 and 500 µM substrate. The reaction mixture was extracted with 300 mL of ethyl acetate and dried under reduced pressure, and was dissolved in HPLC-grade methanol. The samples were filtered through 0.45-µm pore size PTFE filter and subjected to preparative HPLC (Shimadzu) with a C_{18} column (Mightysil RP-18 GP, 150 × 4.6 mm, 5 µm, Kanto Chemical, Japan) for the purification of the respective product peaks.

Analytical methods

The reaction mixture extracted after drying was used for analysis. The dried residue was dissolved in acetonitrile for analysis by Ultra High Performance Liquid Chromatography (UHPLC). The sample was injected into UHPLC and separated using Mightysil Reverse phase C_{18} column (4.6 × 250 mm, 5 µm). Water (A) and acetonitrile (B) were used as mobile phases for separation. The reaction mixture was analyzed using a gradient system of B at 15% for 0 ~ 10 min, 50% for 10 ~ 20 min, 70% for 20 ~ 25 min, and 15% for 25 ~ 40 min at a flow rate of 1 mL/min. Substrates and their products were detected by UV-A at 242 and 245 nm. All the

reaction mixtures were analyzed with SYNAPT G2-S/ACUITY UPLC liquid chromatography quadrupole time-of-light/electrospray ionization mass spectrometry (Waters, Milford, MA, USA) in positive ion mode.

The purified hydroxylated products were dissolved in dimethyl-sulfoxide (DMSO-d_6) and subjected to NMR analyses on 900 MHz using Varain Unity INOVA spectrometer (Varian, Palo Alto, CA, USA). One-dimensional NMRs (^{1}H-NMR and ^{13}C-NMR) were performed by two-dimensional NMR, heteronuclear multiple bond correlation, correlation spectroscopy, rotating-frame overhauser effect spectroscopy (ROESY), and heteronuclear single quantum coherence spectroscopy (HSQC) to delineate the structures when appropriate.

6β-Hydroxyprogesterone. ^{1}H NMR (900 MHz, DMSO-*d*6): δ 5.67 (s, 1H), 5.13 (d, *J* = 2.9 Hz, 1H), 4.16 (q, *J* = 3.0 Hz, 1H), 2.59 (t, *J* = 9.2 Hz, 1H), 2.46 (ddd,*J* = 17.0, 15.0, 5.0 Hz, 1H), 2.21 (dt, *J* = 17.1, 3.5 Hz, 1H), 2.07 (s, 3H), 2.06 – 2.04 (m, 1H), 2.04 – 2.01 (m, 1H), 1.96 (ddd, *J* =13.2, 5.1, 2.8 Hz, 1H), 1.86 (qd, *J* = 10.9, 3.3 Hz, 1H), 1.82 (dt, *J* = 13.6, 3.0 Hz, 1H), 1.65 (tt, *J* = 12.4, 3.8 Hz, 1H), 1.61 (dd, *J* =14.1, 4.3 Hz, 1H), 1.60 – 1.58 (m, 0H), 1.58 (s, 1H), 1.46 – 1.38 (m, 2H), 1.29 (s, 3H), 1.20 – 1.16 (m, 1H), 1.16 – 1.13 (m, 2H), 0.91(td, *J* = 11.3, 4.2 Hz, 1H), 0.58 (s, 3H). ^{13}C NMR (226 MHz, DMSO-d6): δ 209.08 (C20), 199.76 (C3), 169.40 (C5), 125.61 (C4), 71.46 (C6), 63.00 (C17), 55.66 (C14), 53.37 (C9), 43.85 (C13),39.11 (C7), 38.27 (C12), 38.02 (C10), 37.05 (C1), 34.33 (C2), 31.65 (C21), 29.82 (C8), 24.42 (C15), 22.71, 20.99 (C16), 19.39(C11), 13.50 (C18).

6β-Hydroxy,11-ketoprogesterone. ^{1}H NMR (900 MHz, DMSO-d6): δ 5.69 (s, 1H), 5.24 (d, J = 2.9 Hz, 1H), 4.18 (q, J = 2.7 Hz, 1H), 2.82 (t, J = 9.2 Hz, 1H), 2.68 (d, J = 12.4Hz, 1H), 2.60

(ddd, J = 13.4, 5.0, 2.9 Hz, 1H), 2.51 – 2.48 (m, 1H), 2.46 (d, J = 12.4 Hz, 1H), 2.20 (qd, J = 11.3, 3.0 Hz, 1H), 2.17 (dt, J =17.2, 3.4 Hz, 1H), 2.12 (d, J = 11.4 Hz, 1H), 2.09 (dt, J = 13.2, 9.7 Hz, 1H), 2.06 (s, 3H), 1.91 (dt, J = 13.5, 2.9 Hz, 1H), 1.87 (td, J = 11.7,7.2 Hz, 1H), 1.82 – 1.75 (m, 1H), 1.80 – 1.73 (m, 1H), 1.62 (td, J = 14.2, 4.3 Hz, 1H), 1.48 (s, 3H), 1.42 (ddd, J = 13.5, 11.8, 3.2 Hz, 1H),1.26 (qd, J = 11.6, 10.9, 5.3 Hz, 1H), 0.52 (s, 2H). ^{13}C NMR (226 MHz, DMSO-*d*6): δ 209.61 (C11), 208.57 (C20), 199.88 (C3), 167.94 (C5), 126.16 (C4), 70.99 (C6), 61.43 (C9), 61.33 (C17), 56.17(C12), 53.49(C14), 46.71(C13), 39.32(C7), 37.78(C10), 35.79(C1), 34.06(C2), 31.43(C21), 31.02(C8), 23.93(C15), 23.27(C16), 18.92, 14.47(C18).

Results

Hydrogen peroxide tolerance of CYP154C8

Oxidative degradation of heme is a major challenge in H_2O_2-mediated CYP reaction. To determine the effect of H_2O_2 on CYP154C8 reaction, the H_2O_2 tolerance was analyzed in the range of 0.2 ~ 100 mM H_2O_2. The decrease of soret absorbance in an oxidized form of CYP154C8 was monitored at different concentrations of H_2O_2 at intervals up to 30 min. The soret absorbance at different intervals was plotted against time. The soret peak intensity decreased in time during exposure to > 1 mM H_2O_2 concentration (Figure 1). Surprisingly, the heme oxidation rate constant (*K*) was low even at higher concentration of H_2O_2 (Table 1). These data demonstrate that CYP154C8 has high H_2O_2 tolerance even at high (>50 mM) H_2O_2 concentration.

Reaction with NADPH and surrogate redox partner Fdx and Fdr

In vitro reaction reconstituted with spinach surrogate redox partner, cofactor NADPH, glucose-6-phosphate and glucose-6-phosphate dehydrogenase for cofactor regeneration as described in Materials and Methods was highly preferred compared with NADH system and oxidizing agents. The percentage of conversion for all substrates was found to be significantly increased with this system compared with NADH-dependent system (data not shown). Androstenedione and testosterone were completely converted into products. In addition to 16α-hydroxylated product peaks, both the substrate reaction mixtures showed additional peaks in HPLC chromatogram, respectively (Figure 2). LC-MS analysis of the reaction mixture revealed both additional peak as dihydroxylated products of their respective substrates (Figure S1). These dihydroxylated products must have resulted from subsequent hydroxylation of 16α-hydroxylated products in the reaction. To confirm it, 16α-hydroxylated products of androstenedione and testosterone were purified as described in Materials and Methods, and an *in vitro* reactions with 16α-hydroxyandrostenedione and 16α-hydroxytesosterone were carried out instead of androstenedione and testosterone, respectively. The HPLC (Figure S2) and LC-MS (data not shown) analysis confirmed dihydroxylated products of androstenedione and testosterone which were obtained as a result of sequential hydroxylation of 16α-hydroxyandrostenedione and 16α-hydroxytestosterone, respectively. The nandrolone reaction mixture also showed multiple peaks in HPLC chromatograms (Figure S3), where P4 was a major product while others yielded a very low conversion. LC-MS analysis showed P1 as a dihydroxylated product, and the remaining 4 products were found to be hydroxylated at a single position (Figure S4). Androstenedione, testosterone, and nandrolone were never converted to di-hydroxylated products when CYP154C8 was supported by the NADH-dependent system (46). 11-OH progesterone showed a possible major peak of 16α-hydroxylation and a very low additional product peak (Figure S5, inset I).

Both the peaks were identified as monohydroxylated products of 11-hydroxyprogesterone. However, 11-ketoprogesterone was hydroxylated to a single position (Figure S5, inset II). A comparative HPLC and LC-MS analysis with the previous standard showed hydroxylation at C16α-position (46). Progesterone reaction mixture supported by the NADPH-dependent system showed similar product formation pattern compared with the NADH-dependent system based on HPLC analysis (Figure S6, inset I). In our previous report, progesterone in the NADH-dependent system was initially hydroxylated at a C16α position to form 16α-hydroxyprogesterone, which was sequentially hydroxylated at two different positions to yield 6β,16α- dihydroxyprogesterone and 2α,16α-dihydroxyprgestrone (46). The same 16α-hydroxyprogesterone and two dihydroxylated products (6β,16α- dihydroxyprogesterone and 2α,16α-dihydroxyprgestrone) were found to have formed with the NADPH-dependent system too (Figure S6, inset II).

CYP154C8 reaction with (diacetoxyiodo)benzene

In addition to the usual 16α-hydroxyprogesterone product (P1) from progesterone, another monohydroxylated product (P2) was formed when the reaction was carried out with the surrogate oxidant (diacetoxyiodo)benzene which was never observed with another system (Figure 3). NMR-based structural elucidation of the product (P2) revealed as 6β-hydroxyprogesterone. A very low yield of the two dihydroxylated products was detected in the same reaction mixture. Further, when 16α-hydroxpogesterone was used as a substrate instead of progesterone supported by (diacetoxyiodo)benzene, the reaction mixture showed the formation of two different dihydroxylated products with the retention time matching precisely that of the two dihydroxylated products in progesterone reaction mixture (Figure S7). Similarly, HPLC analysis of 11-ketoprogesterone (Figure 4) and 11-hydroxyprogesterone (Figure S8) reaction mixture also

showed two monohydroxylated products, separately. LC-MS analysis (data not shown) revealed both the peaks as monohydroxylated products of respective substrates. The structural elucidation of P2 of 11-ketoprogesterone by NMR showed the hydroxylation at 6β-position, while another product (P1) was identified as 16α-hydroxy,11-ketoprogesterone based on HPLC retention time (Figure S9) and LC-MS (data not shown) comparison with an authentic standard 16α-hydroxy,11-ketoprogesterone. The authentic standard was previously characterized by CYP154C8 supported by the NADH-dependent system (46). A similar peak retention pattern of 11-hydroxyprogesterone was observed, suggesting that these products were also modified at similar position found in 11-ketoprogesterone. Multiple peaks were observed in HPLC chromatogram with testosterone, nandrolone and androstenedione reaction mixture (Figure S10). LC-MS analysis of the reaction mixture showed at least four monohydroxylated products for testosterone (Figure S11A) and nandrolone (Figure S11B) substrates and three monohydroxylated products for androstenedione (Figure S11C) substrate. The major conversion was related to 16α-hydroxylated product for androstenedione (Figure S12A) and testosterone (Figure S12B) identified by HPLC and LC-MS (data not shown) compared with the authentic standards. All other additional products obtained via reactions catalyzed by CYP154C8 were found to be minor, and their selectivity was lower than that of the 16α-hydroxylated product. Progesterone (~ 83%) was the most favored substrate, while all other substrates showed at least 35% conversion yield in the presence of (diacetoxyiodo)benzene (Table 2).

Reaction with H_2O_2

CYP154C8 was active in the presence of high concentration (> 10 mM) of H_2O_2. The optimum conversion of the substrates occurred at ~75 mM H_2O_2. Surprisingly, 16α-hydroxyprogesterone

was the most favored substrate for CYP154C8 in the presence of H_2O_2 (Figure 5). Both products containing 6β,16α- dihydroxyprogesterone and 2α,16α-dihydroxyprgestrone were predominantly observed with an overall conversion of ~ 51 %, while the remaining substrates had a very low conversion (Table S1). Although the percentage of conversion was too low for 11-ketoprogesterone and 11-hydroxyprogesterone, both the substrate reactions showed two monohydroxylated product peaks in HPLC (Figure S13), which were further confirmed by LC-MS (data not shown). The retention times of 11-ketoprogesterone products were similar the previously identified 6β-hydroxy,11-ketoprogesterone and 16α-hydroxy,11-ketoprogesterone obtained in the reactions supported by H_2O_2. The HPLC and LC-MS (data not shown) comparison of progesterone (Figure S14A), androstenedione (Figure S14B) and testosterone (Figure S14C) reaction mixture with the standard showed that the CYP154C8 in the presence of H_2O_2 was region- and stereo-specific to 16α-hydroxylation.

Determination of catalytic efficiency and kinetic parameters

Progesterone was found to be the most favored substrate for CYP154C8 supported by (diacetoxyiodo)benzene. In another reaction when 16α-hydroxyprogesterone was selected as a substrate for CYP154C8 supported by H_2O_2 yielded a higher conversion compared with other steroid substrates. Hence, progesterone and 16α-hydroxyprogesterone were selected to determine the catalytic efficiency and kinetic parameters in the presence of (diacetoxyiodo)benzene and H_2O_2, respectively. The K_m and K_{cat} values for progesterone were estimated at 75.94 ± 10.64 µM and 2.32 ± 0.10 min^{-1}, respectively (Figure 6A). Similarly, 16α-hydroxyprogesterone showed K_m and K_{cat} values of 134.50 ± 17.27 µM and 2.37 ± 0.13 min^{-1}, respectively (Figure 6B). In

addition to the determination of the kinetic parameters, the time-dependent conversion of both substrates has been demonstrated (Figure 7).

Discussion

The *in vitro* reaction with NADPH-dependent system was used to further characterize CYP154C8. The catalytic efficiency of CYP154C8 was not only enhanced with NADPH-dependent system compared with the NADH-dependent system, but also new products were observed. The multi-step oxidation of progesterone by CYP154C8 with NADH-dependent system has been previously been reported (46). The reaction supported by NADPH system showed multi-step oxidation of progesterone, androstenedione, testosterone and nandrolone indicating the preference for NADPH over NADH by CYP154C8. Such product formation in NADPH system also showed the role of alternative redox partner and reducing equivalents in the CYP154C8 catalytic efficiency and product distribution. In addition, it was also established that the choice of appropriate reducing equivalents and surrogate redox partners might play an important role in the catalytic efficiency and product distribution of CYP enzymes (29, 35-40, 48). The multi-step oxidation of steroids by CYP154C8 is novel by any bacterial source of CYPs, although cytochrome $P450_{BioI}$ (CYP107H1) and MycG from bacterial source have already been reported to catalyze the multi-step oxidation of fatty acids and mycinamycin-IV, respectively (35, 49). Some of the CYPs like CYP11A1, CYP17A1, CYP19A1 and CYP24A1 from the mammalian source are widely known to catalyze the multi-step oxidation of steroids (50-53).

In addition to the 16α-hydroxylated products of the substrate progesterone and 11-ketoprogesterone, the formation of 6β-hydroxylated products from the both substrates supported by oxygen surrogate (diacetoxyiodo)benzene was unusual because such products were never observed with NAD(P)H-dependent system, although a very low conversion occurred in the presence of H_2O_2 (Scheme 2). However, such product formation in the presence of only oxygen surrogates is not clear, allosteric effects of interactions with redox partners affect the CYP activity and product distribution. Recently, it was reported that CYP17A1 yields different products in the presence of iodosobenzene and NADPH-P450 reductase, to form compound I (29). The effect of cytochrome b5 on the catalytic activity and product formation of CYPs has been widely studied, and shown to induce the activity of specific CYPs (54, 55). In another experiment, MycG, a CYP derived from bacterial source showed altered catalytic type in conjunction with an alternate surrogate redox partner, which highlights the role of variant redox partner in protein-protein interaction in the catalytic activity of CYP enzyme (35). In addition to electron transfer, the complex of CYP101A1 with its natural redox partner protein, Pdx demonstrates an important allosteric regulatory role of these redox partner proteins bound with CYP (56, 57). Few CYPs are known to possess activity in the presence of (diacetoxyiodo)benzene. Mammalian and bacterial CYPs such as CYP5A1, CYP17A1, CYP121, CYP101A1 ($P450_{cam}$) and CYP106A2 are known to show catalytic activity in the presence of iodobenzene as a single oxygen donor (30, 58-61). The oxygenation mechanism supported by (diacetoxyiodo)benzene might be similar to iodosobenzene, probably mediated via a two-electron transfer of a single oxygen atom from oxidant to ferric CYP to generate compound I, which is involved in substrate monoxygenation (58). CYP154C8 hydroxylation occurred usually at the α-face of D-ring to steroid substrates. Interestingly, the hydroxylation occurred at the β-

face of progesterone and 11-ketoprogesterone and regioselectivity switched from D-ring to B-ring. As reported previously, the 16α-hydroxyprogesterone was sequentially hydroxylated at 2α and 6β position to yield the respective dihydroxylated product of progesterone (46). CYP17A1 unusual to its function hydroxylated at 6β-position when 16α,17α-dihydroxyprogesterone was used as a substrate, which was attributed due to the presence of two hydroxyl groups on the 16α- and 17α-position (29). The switch in hydroxylation from D-ring to B-ring by CYP154C8 in presence of (diacetoxyiodo)benzene and H_2O_2 indicates the effect of oxidation system. Although, NADPH as well as NADH-dependent system efficiently supported the CYP154C8 activity, they never induced formation of 6β-hydroxylated product from the substrate progesterone and 11-ketoprogesterone or/with any other substrates, suggesting the role of a redox partner in protein-protein interactions for modulating the specificity of CYP. In addition, the functional groups such as hydroxyl or the carbonyl group in the substrate may also influence the selectivity of hydroxylation, although such switch in selectivity of different CYPs may not be the same (35, 39). The B-ring hydroxylation by CYP154C8 supported by (diacetoxyiodo)benzene and H_2O_2 is unclear. However, the hydroxylation at C16α-position of progesterone might play a key role in subsequent hydroxylation to A-ring and B-ring yielding 2α,16α-dihydroxyprogesterone and 6β,16α-dihydroxyprogesterone, respectively.

The peroxide shunt pathway uses H_2O_2 (or the oxygen donors) to drive CYPs, and represents one of the efficient ways of using these enzymes for industrial application. However, the oxidative degradation of heme by peroxide has been a major issue (15, 62). The activity of CYP154C8 in the presence of high concentration of H_2O_2 is interesting and surprising. CYP154C8 displayed comparative tolerance to H_2O_2, although the *in vitro* activity was only observed with > 10 mM H_2O_2. More importantly, the heme oxidation rate constant (*K*) of

CYP154C8 even at high concentration (100 mM) of H_2O_2 was consistently low (K > 0.6 min^{-1}). A widely studied CYP, CYP152L1 uses H_2O_2 to catalyze reactions and the recent studies supporting its hydrogen peroxide tolerance showed greater H_2O_2 tolerance than other CYPs (CYP121A1, P450 BM3 and CYP51B1) (63). The comparison of previously reported heme oxidation rate constant (K) of CYP152L1 and CYP154C8 showed a higher tolerance of CYP154C8 to H_2O_2 for 30 min, while other CYPs were incubated for 1 h with different concentrations of H_2O_2. The activity of CYP154C8 in the presence of H_2O_2 with steroid substrates was low; in contrast, the elevated activity towards 16α-hydroxyprogesterone was unusual. 6β-hydroxyprogesterone and 16α-hydroxyprogesterone are pharmaceutically important compounds. 6β-hydroxyprogesterone is used as an intermediate for the synthesis of anticancer compound 6β,14α-dihydroxyandrost-4-ene-3,17-dione, an inhibitor of the growth of breast cancer cells and an inhibitor of the 5α-reductase activity in male rats, representing a potential lead for the development of drugs against prostate cancer (64-67).

In conclusion, CYP154C8 catalyzes the sequential oxidation of steroid substrates that prefers NADPH over NADH-dependent system. In addition, the use of alternative surrogate redox partners and reducing equivalents might alter the catalytic efficiency and product distribution. The unexpected change in product distribution pattern of steroid substrates observed with NADPH, (diacetoxyiodo)benzene and H_2O_2 systems indicates the altered role of active oxygen species in P450-mediated oxidation reactions. The optimum activity of CYP154C8 in the presence of high concentrations of H_2O_2 is unusual and warrants further studies.

Acknowledgments

This research was supported by a grant (NRF-2016R1D1A3B03933814) of the Basic Science Research Program through the National Research Foundation of Korea (NRF) funded by the Ministry of Education, Science and Technology, Republic of Korea. In addition, this work was supported by the Korea Polar Research Institute (grant no. PE18210). We would like to thank Division of Magnetic Resonance, Korea Basic Science Institute, Ochang, Chungbuk, Korea for NMR analyses.

Conflict of interest

The authors declare that they have no conflict of interest.

References

1. http://www.drnelson.uthsc.edu/cytochromeP450.html.
2. F.P. Guengerich, A.W. Munro, *J. Biol. Chem*. **2013**, 288, 17065-17073.
3. A.V. Pandey, C.E. Flück, *Pharmacol. Ther*. **2013**, 138, 229-254.
4. K.J. McLean, D. Luciakova, J. Belcher, K.L. Tee, A.W. Munro, *Adv. Exp. Med. Biol.* **2015**, 851, 299-317.
5. L.O. Narhi, A.J. Fulco, *J. Biol. Chem.* **1986**, 261, 7160-7169.
6. R.D. Mot, A.H. Parret, *Trends Microbiol*. **2002**, 10, 502-508.

7. A.J. Warman, J.W. Robinson, D. Luciakova, A.D. Lawrence, K.R. Marshall, M.J. Warren, M.R. Cheesman, S.E. Rigby, A.W. Munro, K.J. McLean, *FEBS J.* **2012**, 279, 1675-1693.
8. M. Tavanti, J.L. Porter, S. Sabatini, N.J. Turner, S.L. Flitsch, *ChemCatChem* **2018**, 10, 1042.
9. D. Minerdi, S.J. Sadeghi, G.D. Nardo, F. Rua, P. Castignano, G. Gilardi, *Mol. Microbiol.* **2015**, 95, 539-554.
10. Y. Yin, H. Yu, Z. Luan, R. Li, P. Ouyang, J. Liu, J. Xu, *ChemBioChem* **2014**, 15, 2443-2449.
11. J.L. Porter, J. Manning, S. Sabatini, M. Tavanti, N.J. Turner, S.L. Flitsch, *ChemBioChem* **2018**, 19, 513.
12. R. Bernhardt, *J. Biotechnol.* **2006**, 124, 128-145.
13. B. Zhao, L. Lei, D.G. Vassylyev, X. Lin, D.E. Cane, S.L. Kelly, H. Yuan, D.C. Lamb, M.R. Waterman, *J. Biol. Chem.* **2009**, 284, 36711-36719.
14. Q. Cheng, D.C. Lamb, S.L. Kelly, L. Lei, F.P. Guengerich, *J. Am. Chem. Soc.* **2010**, 132, 15173-15175.
15. P.R. Ortiz de Montellano, *Chem. Rev.* **2010**, 110, 932-948.
16. I. Matsunaga, A. Ueda, T. Sumimoto, K. Ichihara, M. Ayata, H. Ogura, *Arch. Biochem. Biophys.* **2001**, 394, 45-53.
17. M. Girhard, S. Schuster, M. Dietrich, P. Dürre, V.B. Urlacher, *Biochem. Biophys. Res. Commun.* **2007**, 362, 114-119.
18. M.A. Rude, T.S Baron, S. Brubaker, M. Alibhai, S.B. Del Cardayre, A. Schirmer, *Appl. Environ. Microbiol.* **2011**, 77, 1718-1727.

19. I. Matsunaga, M. Yamada, E. Kusunone, T. Miki, K. Ichihara, *J. Biochem*. **1998**, 124, 105-110.

20. O. Shoji, T. Fujishiro, H. Nakajima, M. Kim, S. Nagano, Y. Shiro, Y. Watanabe, *Angew. Chem. Int. Ed.* **2007**, 46, 3656-3659.

21. P.C. Cirino, F.H. Arnold, *Angew. Chem. Int. Ed. Engl.* **2003**, 42, 3299-3301.

22. S. Kumar, C. Chen, D. Waxman, *J. Biol. Chem.* **2005**, 280, 19569-19575.

23. R.K. Behera, S. Goyal, S. Mazumdar, *J. Inorg. Biochem.* **2010**, 104, 1185-1194.

24. N. Ma, Z. Chen, J. Chen, J. Chen, C. Wang, H. Zhou, L. Yao, O. Shoji, Y. Watanabe, Z. Cong, *Angew. Chem. Int. Ed. Engl.* **2018**, 57, 7628.

25. H. Onoda, O. Shoji, Y. Watanabe, *Dalton Trans.* **2015**, 44, 15316-15323.

26. A. Berg, K. Carlstrom, J.-A. Gustafsson, M. Ingelman-Sundberg, *Biochem. Biophys. Res. Commun.* **1975**, 66, 1414-1423.

27. J.-A. Gustafsson, J. Bergman, *FEBS Lett*. **1976**, 70, 276-280.

28. F. Lichtenberger, W. Nastainczyk, V. Ullrich, *Biochem. Biophys. Res. Commun.* **1976**, 70, 939-946.

29. F.K. Yoshimoto, E. Gonzalez, R.J. Auchus, and F.P. Guengerich, *J. Biol. Chem*. **2016,** 291, 17143-17164.

30. J.K. Kulig, C. Spandolf, R. Hyde, A.C. Ruzzini, L.D. Eltis, G. Gronberg, M.A. Hayes, G. Grogan, *Bioorg. Med. Chem*. **2015**, 23, 5603-5609.

31. K.J. McLean, M. Hans, B. Meijrink, W.B. van Scheppingen, A. Vollebregt, K.L. Tee, J.M van der Laan, D. Leys, A.W. Munro, M.A. van den Berg, *Proc. Natl. Acad. Sci*. **2015**, 112, 2847-2852.

32. T. Makino, Y. Katsuyama, T. Otomatsu, N. Misawa, Y. Ohnishi, *Appl. Environ. Microbiol.* **2014**, 80, 1371-1379.

33. Y. Khatri, M. Ringle., M. Lisurek, J.P. von Kries, J. Zapp, R. Bernhardt, *ChemBioChem* **2016**, 17, 90.

34. R. Bernhardt, V.B. Urlacher, *Appl. Microbiol. Biotechnol*. **2014**, 98, 6185-6203.

35. W. Zhang, Y. Liu, J. Yan, S. Cao, F. Bai, Y. Yang, S. Huang, L. Yao, Y. Anzai, F. Kato, L.M. Podust, D.H. Sherman, S. Li, *J. Am. Chem. Soc*. **2014**, 136, 3640-3646.

36. R.C. Tuckey, K.J. Cameron, *Biochim. Biophys. Acta.* **1993**, 1163, 185-194.

37. Y. Khatri, A. Schifrin, R. Bernhardt, *FEBS Lett*. **2017**, 591, 1126-1140.

38. S.G. Bell, A. Dale, N.H. Rees, L.L. Wong, *Appl. Microbiol. Biotechnol*. **2010**, 86, 163-175.

39. E. Jung, B.G. Park, M.M. Ahsan, J. Kim, H. Yun, K.Y. Choi, B.G. Kim, *Appl. Microbiol. Biotechnol.* **2016**, 100, 10375-10384.

40. W. Yang, S.G. Bell, H. Wang, W. Zhou, N. Hoskins, A. Dale, M. Bartiam, L.L. Wong, Z. Rao, *J. Biol. Chem*. **2010**, 285, 27372-27384.

41. F.M. Kiss, D. Schmitz, J. Zapp, *Appl Microbiol Biotechnol.* **2015**, 99, 8495.

42. H. Agematu, N. Matsumoto, Y. Fujii, H. Kabumoto, S. Doi, K. Machida, J. Ishikawa, A. Arisawa, *Biosci. Biotechnol. Biochem.* **2006**, 70, 307-311.

43. I.K. Jóźwik, F.M. Kiss, Ł. Gricman, A. Abdulmughni, E. Brill, J. Zapp, J. Pleiss, R. Bernhardt, A.W. Thunnissen, *FEBS J.* **2016**, 283, 4128-4148.

44. P. Bracco, D.B. Janssen, A. Schallmey, *Microb. Cell Fact.* **2013**, 12, 95.

45. S.G. Salamanca-Pinzon, Y. Khatri, Y. Carius, L. Keller, R. Müller, C.R. Lancaster, R. Bernhardt, *FEBS Lett.* **2016**, 590, 1838-1851.

46. B. Dangi, K.H. Kim, S.H. Kang, T.J. Oh. *ChemBioChem* **2018**, 19, 1066-1077.

47. S. Bhattarai, K. Liou, T.J. Oh, *Arch. Biochem. Biophys.* **2013**, 539, 63-69.

48. Y. Anzai, S. Li, R.M. Chaulagain, K. Kinoshita, F. Kato, J. Montgomery, D.H. Sherman, *Chem. Biol*. **2008**, 15, 950.

49. M.J. Cryle, J.J. De Voss, *Chem. Commun*, **2004**, 86-87.

50. R. Davydov, N. Strushkevich, D. Smil, A. Yantsevich, A. Gilep, S. Usanov, B.M. Hoffman, *Biochemistry* **2015**, 54, 7089-7097.

51. J.R. Berrie, R.A. Williams, K.E. Smith, *J. Steroid Biochem. Mol. Biol.* **1999**, 71, 153-165.

52. Y. Osawa, K. Shibata, D. Rohrer, C. Weeks, W.L. Duax, *J. Am. Chem. Soc.* **1975**, 97, 4400-4402.

53. M.J. Beckman, P. Tadikonda, E. Werner, J. Prahl, S. Yamada, H.F. DeLUCA *Biochemistry*. **1996**, 35, 8645-8472.

54. L. Waskell. J.-J.P. Kim, (Ortiz de Montellano, P. R., ed) pp. 33-60, *Springer*, New York, **2015**.

55. M.R. Bhatt, Y. Khatri, R.J. Rodgers, L.L Martin, *J. Steroid Biochem. Mol. Biol*. **2017**, 170, 2-18.

56. Y. Hiruma, M.A. Hass, Y. Kikui, W.M. Liu, B. Olmez, S.P. Skinner, A. Blok, A. Kloosterman, H. Koteishi, F. Lohr, H. Schwalbe, M. Nojiri, M. Ubbink, *J. Mol. Biol.* **2013**, 425, 4353-4365.

57. S. Tripathi, H. Li, T.L. Poulos, *Science* **2013**, 340, 1227-1230.

58. E.G. Hrycay, S.M. Bandiera, *Arch. Biochem. Biophys.* **2012**, 522, 71-89.

59. K. Dornevil, I. Davis, A.J. Fielding, J.R. Terrell, L. Ma, A. Liu, *J. Biol. Chem.* **2017**, 292, 13645-13657.

60. M.H. Gelb, D.C. Heimbrook, P. Mälkönen, S.G. Sligar, *Biochemistry* **1982**, 21, 370-377.

61. A. Berg, M. Ingelman-Sundberg, J.A. Gustafsson, *J. Biol. Chem*. **1979**, 254, 5264-5271.

62. A.W. Munro, H.M. Girvan, A.E. Mason, A.J Dunford, K.J McLean, *Trends Biochem. Sci*. **2013**, 38, 140-150.

63. S. Matthews, K.L. Tee, N.J. Rattray, K.J. McLean, D. Leys, D.A. Parker, R.T. Blankley, A.W. Munro, *FEBS Lett*. **2017**, 591, 737-750.

64. U. Raju, H.L. Bradlow, M. Levitz, *Ann. N. Y. Acad. Sci*. **1990**, 586, 83-87.

65. J. Marcos, W.Y. Craig, G.E. Palomaki, E.M. Kloza, J.E. Haddow, M. Roberson, L.A. Bradley, C.H. Shackleton, *Prenat. Diagn.* **2009**, 29, 771-780.

66. A. Yamada, M. Yamada, Y. Fujita, T. Nishigami, K. Nakasho, K. Uematsu, *J. Biol. Chem.* **2001**, 276, 4604-4610.

67. K.E. Smith, S. Latif, D.N. Kirk, *J. Steroid Biochem.* **1990**, 35, 115-120.

10.1002/cbic.201800284

519 **Table 1.** Rates of heme oxidation constant (*K*) and absorbance amplitude (*A*) for heme soret peak
520 absorbance change at 417 nm of CYP154C8. Data were fitted in one-phase exponential decay
521 using GraphPad Prism 6. ND denotes "not determined" due to small amplitudes of heme
522 absorbance change.

H_2O_2 (mM)	*K* (min^{-1})	*A*
0.2	ND	0.010
1	0.18 ± 0.040	0.016
3	0.09 ± 0.005	0.075
5	0.02 ± 0.020	0.092
20	0.12 ± 0.015	0.233
50	0.18 ± 0.012	0.235
75	0.51 ± 0.004	0.227
100	0.18 ± 0.050	0.223

523

Table 2. The conversion percentage of steroid substrates and selectivity of product formation supported by (diacetoxyiodo)benzene. The table also shows the retention times of substrate and their respective products. The product quantification was performed by correlating the peak area of the products with the combined peak area of products and substrate. 16-OHP, 16α-hydroxyprogesterone; 6-OHP, 6β-hydroxyprogesterone; 16-OHA, 16α-hydroxyandrostenedione; and 16-OHT, 16α-hydroxyandrostenedione. P1-P4 represent the different products formed in the reactions with respective substrates.

Substrates	Conversion (%)	Selectivity (%)	Retention time (min)
Progesterone	83.3	16α-OHP (70.0), 6β-OHP (25.0)	S (26.6), 16-OHP (14.6), 6-OHP (16.8)
Androstenedione	36.2	16α-OHA (66.0), P1 (9.4), P2 (9.5), P3 (15.0)	S (18.7), 16-OHA (13.7), P1 (13.2), P2 (13.9), P3 (14.7)
Testosterone	37.5	16α-OHT (76.0), P1 (3.0), P2 (17.0), P3 (4.0)	S (17.2), 16α-OHT (12.1), P1 (11.2), P2 (11.9), P3 (13.8)
Nandrolone	68.6	P1 (13.5), P2 (31.5), P3 (50.4) P4 (4.3)	S (16.0), P1 (10.2), P2 (10.8), P3 (11.2), P4 (13.2)
11-Hydroxyprogesterone	69.0	P1 (61.8) P2 (38.2)	S (15.6), P1 (10.7), P2 (11.0)
11-Ketoprogesterone	50.3	P1 (75.0), P2 (25.0)	S (17.7), P1 (12.5), P2 (13.0)
16α-Hydroxyprogesterone	14.0	P1 (9.5), P2 (4.5)	S (14.6), P1 (11.3), P2 (12.0)

10.1002/cbic.201800284

532 **Scheme 1.** Steroids used as substrates for further characterization of CYP154C8.

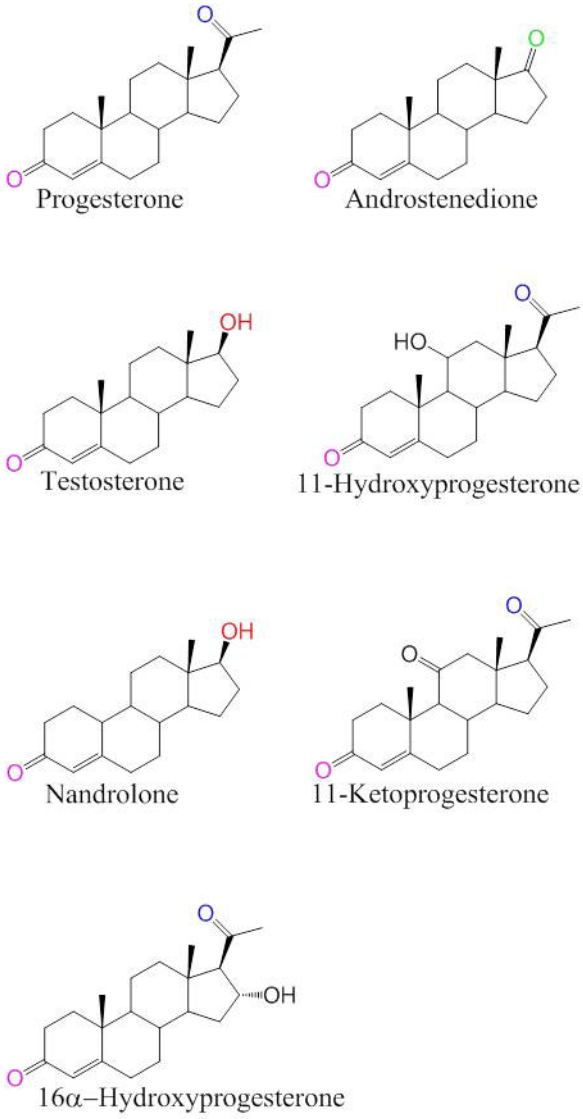

533

534 **Scheme 2.** Hydroxylation of progesterone (**A**) and 11-ketoprogesterone (**B**) mediated by
535 CYP154C8.

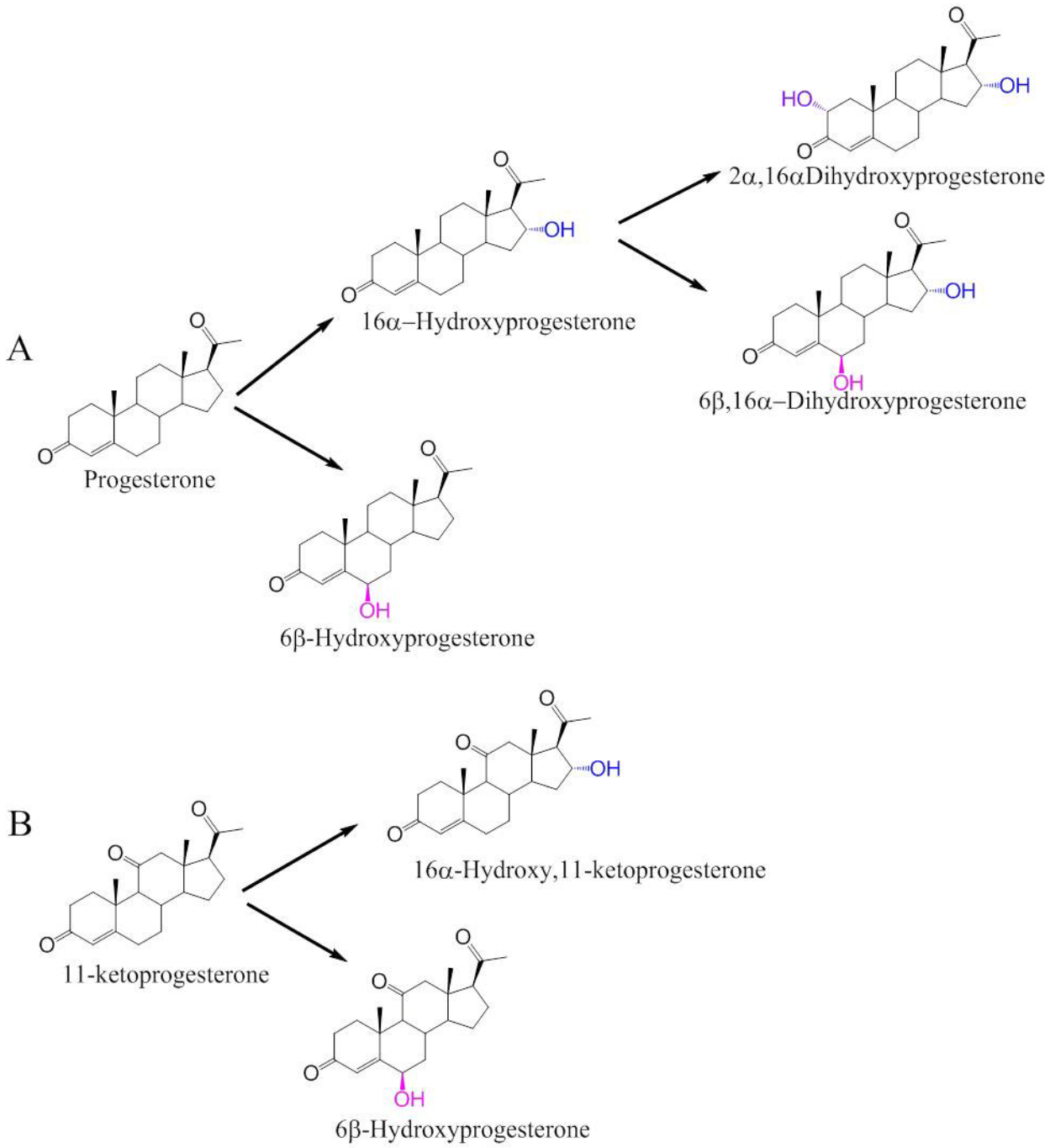

536

10.1002/cbic.201800284

537 **Figure 1.** H_2O_2 tolerance by CYP154C8. The spectra show the absorbance for 30 min at the
538 interval of 1.5 min at H_2O_2 concentration. **A,** 1 mM; **B,** 3 mM; **C,** 5 mM; **D,** 20 mM; **E,** 50 mM;
539 and **F,** 100 mM.

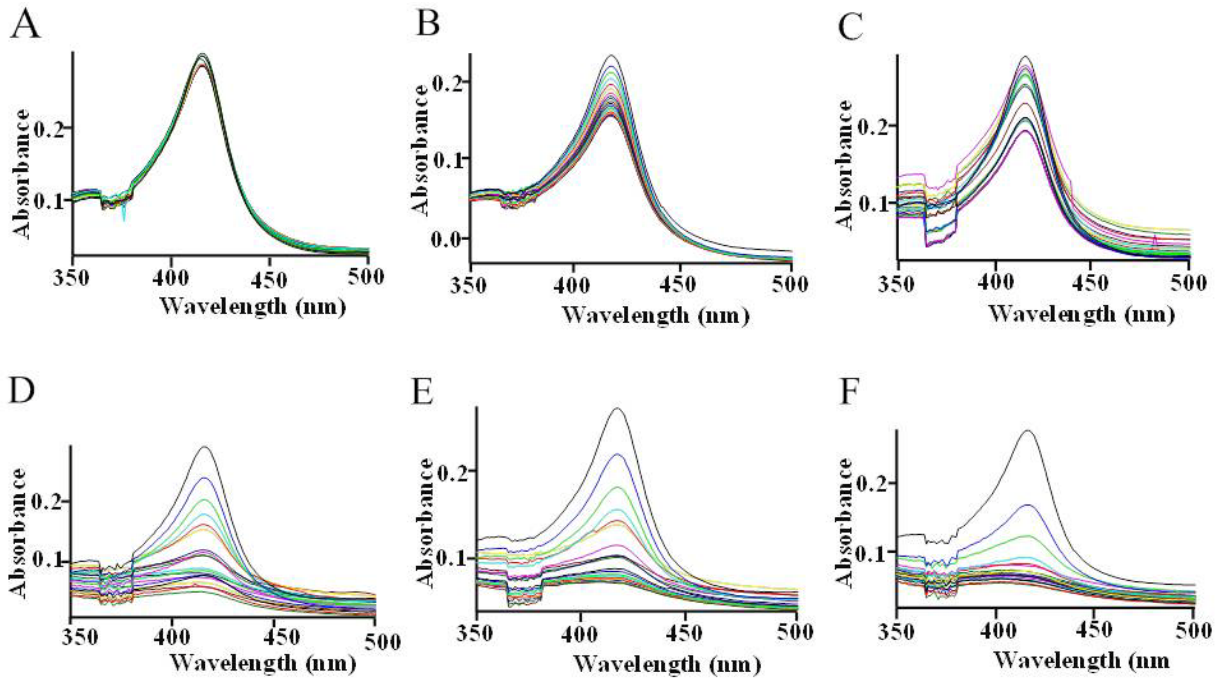

540
541

542 **Figure 2.** HPLC chromatogram of the reaction mixture. Androstenedione (**A**) and testosterone
543 (**B**) supported by NADPH-dependent system. Insets I and II display the chromatograms of
544 reaction and control of respective substrate, respectively. Di-OHA and di-OHT denote
545 dihydroxyandrostenedione and dihydroxytesoterone, respectively.

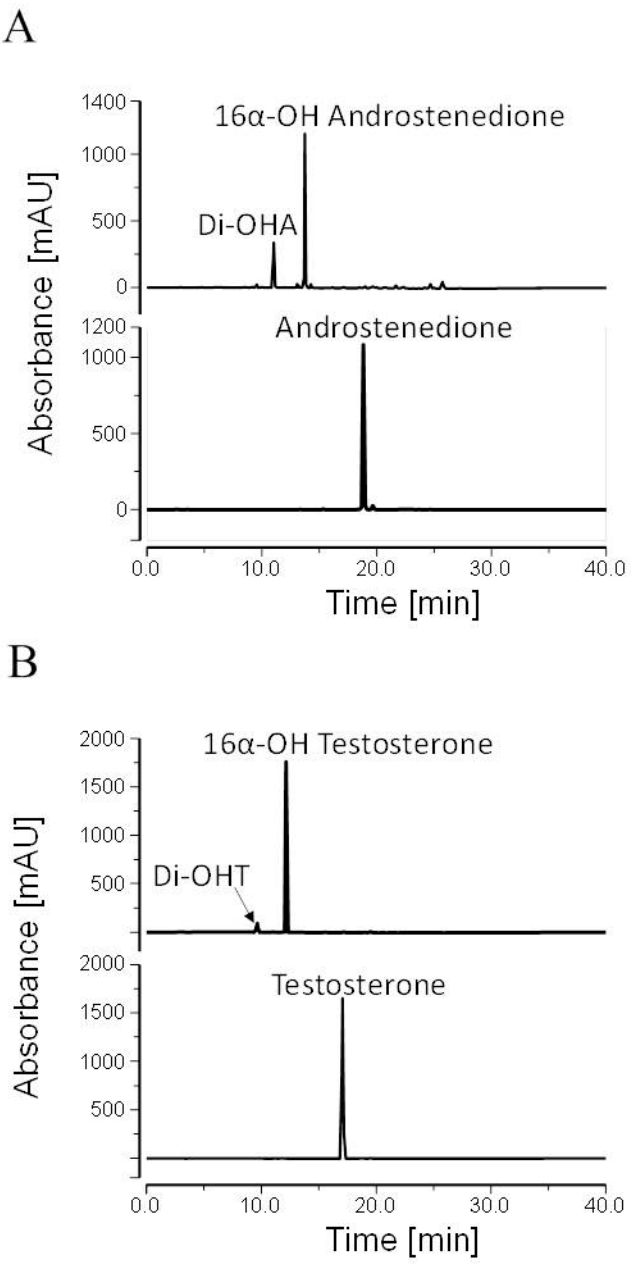

546

10.1002/cbic.201800284

547 **Figure 3.** HPLC chromatogram of the progesterone reaction mixture in the presence of
548 (diacetoxyiodo)benzene (inset I) and NADPH (inset II). 2α,16α-di-OHP and 6β,16α-di-OHP
549 indicate 2α,16α-dihydroxyprogesterone and 6β,16α-dihdyroxyprogesterone, respectively.

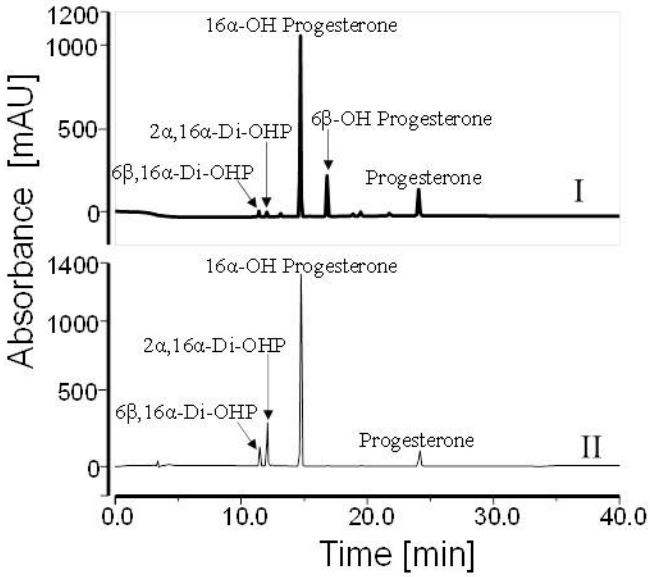

550

10.1002/cbic.201800284

551 **Figure 4.** HPLC chromatogram of the 11-ketoprogesterone reaction mixture in the presence of
552 (diacetoxyiodo)benzene (inset I) and NADPH (inset II). 6-OH and11-KP indicate 6β-hydroxy
553 and 11-ketoprogesterone, respectively.

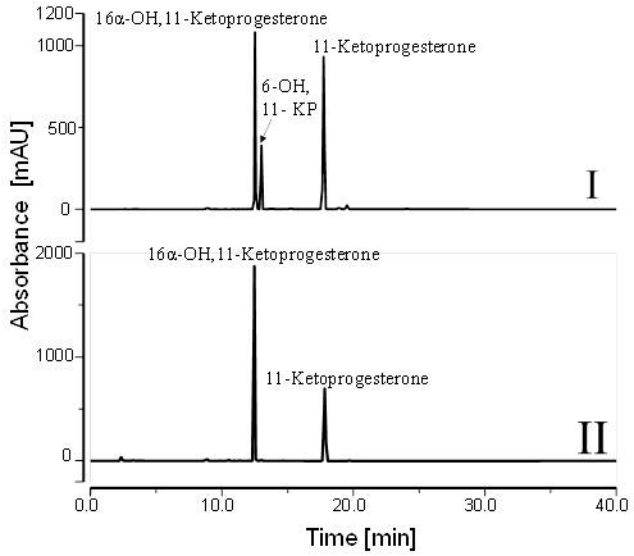

554

10.1002/cbic.201800284

555 **Figure 5**. HPLC chromatogram of 16α-hydroxyprogesterone reaction mixture (inset I) in the
556 presence of H_2O_2 and standard 16α-hydroxyprogesterone (inset II). 2α,16α-di-OHP and 6β,16α-
557 di-OHP stand for 2α,16α-dihydroxyprogesterone and 6β,16α-dihdyroxyprogesterone,
558 respectively. The *in vitro* reaction was carried out in the presence of 3 µM CYP154C8, 0.5 mM
559 substrate, and 75 mM H_2O_2 for 2 h at 30°C.

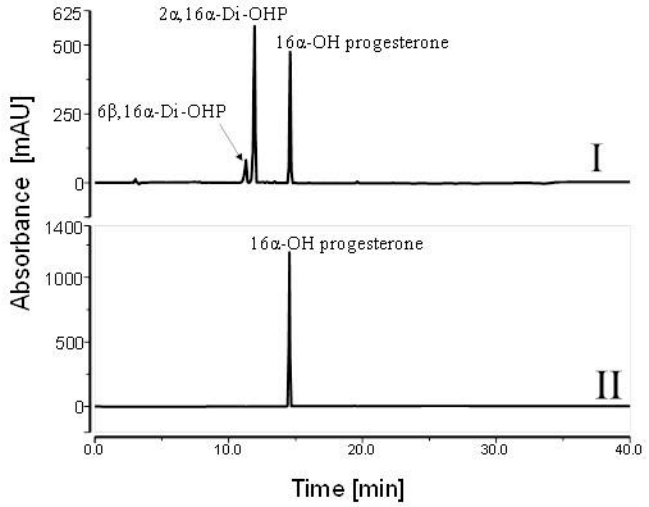

560

561 **Figure 6.** (**A**) Hyperbolic fit of 16α-hydroxyprogesterone in the presence of
562 (diacetoxyiodo)benzene. (**B**) Hyperbolic fit of 2α,16α-dihydroxyprogesterone and 6β,16α-
563 dihydroxyprogesterone in the presence of H_2O_2.

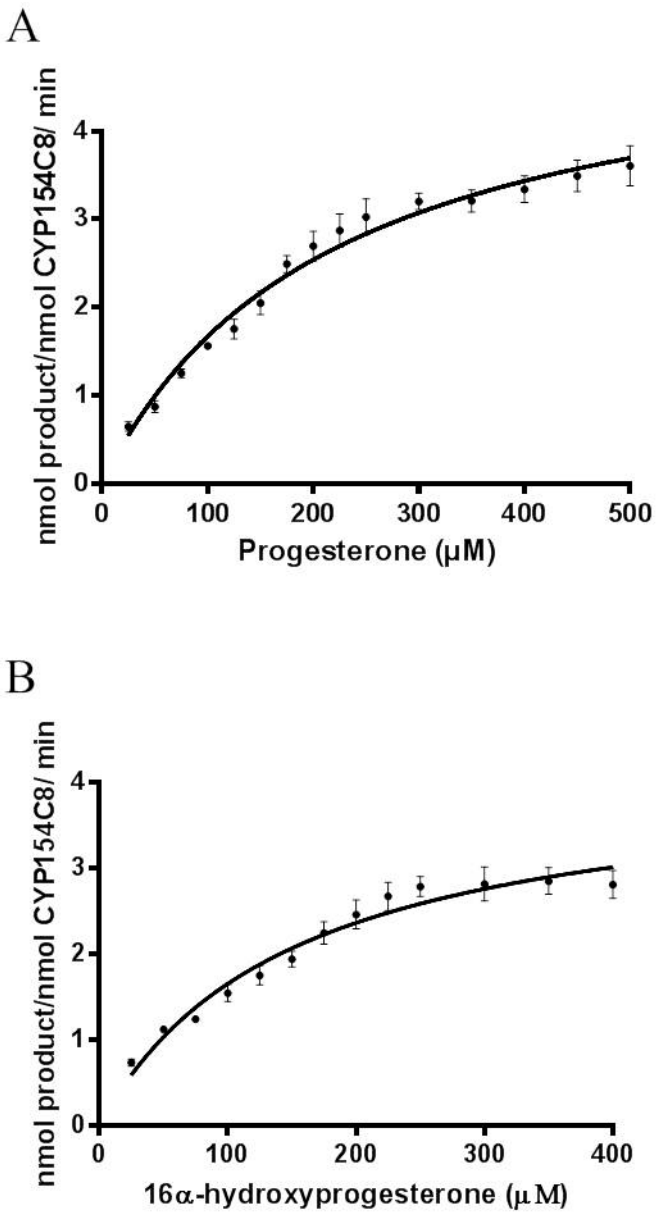

564

565 **Figure 7.** Time-dependent conversion of 16α-hydroxyprogesterone (**A**) and progesterone (**B**) in
566 the presence of H_2O_2 and (diacetoxyiodo)benzene, respectively. The reactions were carried out
567 with 1 μM CYP154C8 and 0.5 mM substrate at 30°C for different time intervals (1 ~ 60 min).
568 The reactions involving 16α-hydroxyprogesterone and progesterone were initiated with 75 mM
569 H_2O_2 and 2 mM (diacetoxyiodo)benzene, respectively.

10.1002/cbic.201800284

A

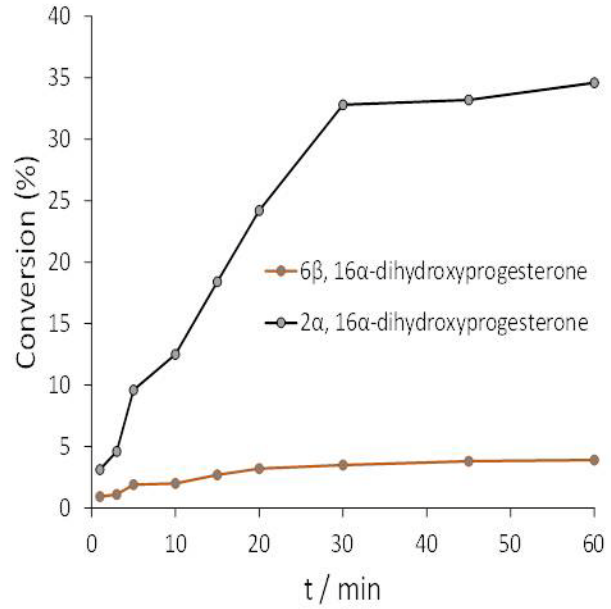

B

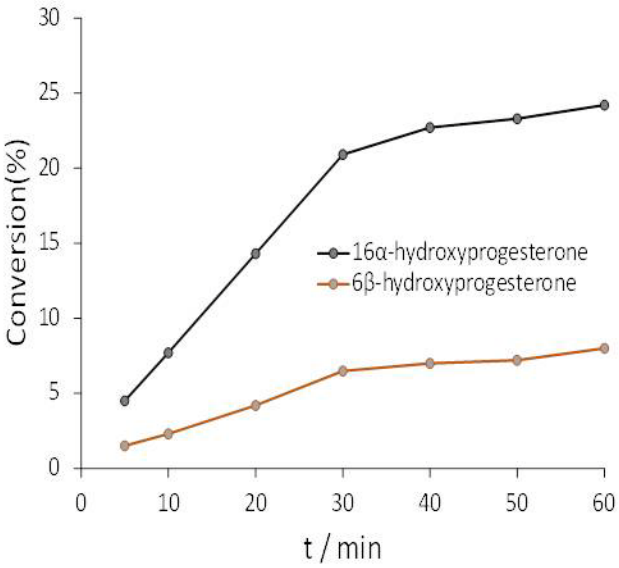

570

10.1002/cbic.201800284

571 **Text for the table of contents**

572 **Altered activity:** CYP154C8 reconstituted with variant redox partner dislayed an altered
573 catalytic activity. In addition to 16α-hydroxylation, progesterone and 11-ketoprogesterone were
574 hydroxylated at 6β-position in the reaction supported by diacetoxyiodobenzene (PIDA), unusual
575 to the reaction supported by NADPH- and NADH-dependent system. CYP154C8 also showed
576 the conversion of steroids at high concentration of H_2O_2 and showed high H_2O_2 tolerance.

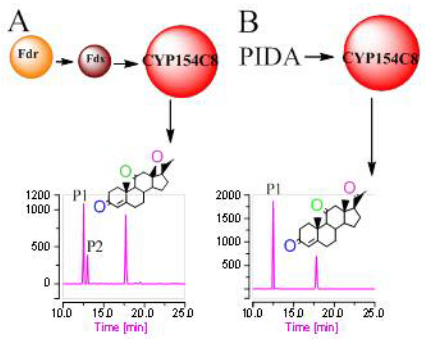

577